REPORT

OPEN ACCESS

www.the-innovation.org

Billions of people exposed to increasing heat but decreasing greenness from 2000 to 2022

Tingting Ye,[1,2,8] Rongbin Xu,[1,2,8] Wenzhong Huang,[2] Zhengyu Yang,[2] Pei Yu,[2] Wenhua Yu,[2] Yanming Liu,[2] Yao Wu,[2] Bo Wen,[2] Yiwen Zhang,[2] Jaime E. Hart,[3,4] Mark Nieuwenhuijsen,[5,6,7] Michael J. Abramson,[2] Yuming Guo,[2,*] and Shanshan Li[2,*]

*Correspondence: yuming.guo@monash.edu (Y.G.); shanshan.li@monash.edu (S.L.)

Received: August 30, 2024; Accepted: March 4, 2025; Published Online: March 7, 2025; https://doi.org/10.1016/j.xinn.2025.100870

GRAPHICAL ABSTRACT

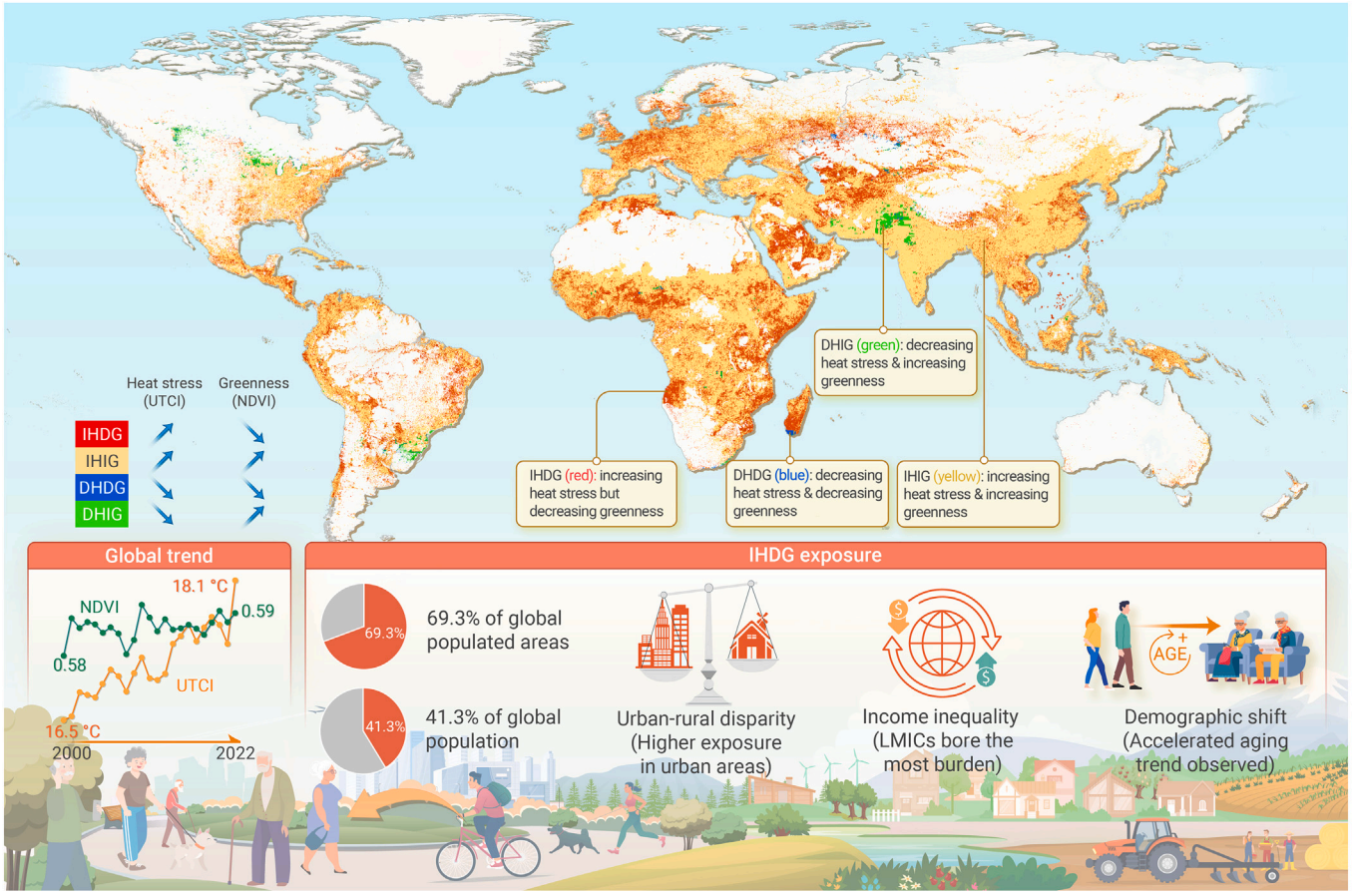

PUBLIC SUMMARY

- 69.3% of global populated areas experienced increasing heat but decreasing greenness (IHDG).
- 41.3% of the global population (~2.9 billion people) was exposed to IHDG.
- Low- and middle-income countries bore 85% of this burden, with urban areas more affected than rural ones.
- An accelerated aging trend was observed in populations exposed to IHDG.

OPEN ACCESS

REPORT

The Innovation

Billions of people exposed to increasing heat but decreasing greenness from 2000 to 2022

Tingting Ye,[1,2,8] Rongbin Xu,[1,2,8] Wenzhong Huang,[2] Zhengyu Yang,[2] Pei Yu,[2] Wenhua Yu,[2] Yanming Liu,[2] Yao Wu,[2] Bo Wen,[2] Yiwen Zhang,[2] Jaime E. Hart,[3,4] Mark Nieuwenhuijsen,[5,6,7] Michael J. Abramson,[2] Yuming Guo,[2,*] and Shanshan Li[2,*]

[1]School of Medicine, Chongqing University, Chongqing 400044, China

[2]Climate, Air Quality Research Unit, School of Public Health and Preventive Medicine, Monash University, Melbourne, VIC 3004, Australia

[3]Department of Environmental Health, Harvard T. H. Chan School of Public Health, Boston, MA 02115, USA

[4]Channing Division of Network Medicine, Department of Medicine, Brigham and Women's Hospital and Harvard Medical School, Boston, MA 02115, USA

[5]ISGlobal, 08003 Barcelona, Spain

[6]Universitat Pompeu Fabra (UPF), 08003 Barcelona, Spain

[7]CIBER Epidemiología Y Salud Pública (CIBERESP), 28029 Madrid, Spain

[8]These authors contributed equally

*Correspondence: yuming.guo@monash.edu (Y.G.); shanshan.li@monash.edu (S.L.)

Received: August 30, 2024; Accepted: March 4, 2025; Published Online: March 7, 2025; https://doi.org/10.1016/j.xinn.2025.100870

Citation: Ye T., Xu R., Huang W., et al., (2025). Billions of people exposed to increasing heat but decreasing greenness from 2000 to 2022. The Innovation **6(5)**, 100870.

Rising heat stress due to climate warming poses a significant threat to human health, and greenness offers a nature-based solution to mitigate heat-related health impacts and enhance resilience. Although global greenness has increased, it remains unclear whether these trends align with the population's heat mitigation needs. In this study, we integrated spatially resolved demographic data with satellite-derived greenness metric and reanalysis-based heat stress data to construct a global profile of joint exposure at 1 × 1 km resolution from 2000 to 2022. We found that 69.3% of global populated areas and 41.3% of the global population (~2.9 billion people) were exposed to increasing heat stress but decreasing greenness (IHDG), representing the most concerning situation for heat mitigation. Urban populations were disproportionately affected, with 50.8% exposed compared to 27.1% in rural areas. Low- and middle-income countries exhibited more pronounced trends of increasing heat stress and bore the greatest burden from IHDG, accounting for 85% of total exposed populations. Moreover, there was a notable demographic shift in IHDG-exposed populations toward older groups, exacerbating the heat mitigation crisis. This study advances the understanding of the joint dynamics of heat stress and greenness and provides a profile of population exposure at a fine grid level. By highlighting the scale of IHDG conditions, our findings emphasize the urgent need to address this environmental challenge and a significant opportunity for improving greenness to mitigate increasing heat globally. The spatially detailed assessment maps offer essential data for informed decision-making.

INTRODUCTION

Heat exposure has increased in frequency, duration, and intensity, with projections indicating further exacerbations of this pattern as global warming intensifies.[1] Exposure to extreme heat is associated with numerous adverse health consequences, including increased mortality, hospital admissions, emergency department visits, and adverse pregnancy and birth outcomes.[2] Globally, heat contributes to approximately 489,075 premature deaths annually.[3] The urban heat island effect, combined with the heightened vulnerability of elderly populations to heat, exacerbates these health impacts.[4] Rapid urbanization and population aging further complicate heat mitigation efforts, particularly in low- and middle-income countries (LMICs), where adaptative capacity is limited.[5,6]

Nature-based solutions, particularly urban green spaces, have been widely recognized as effective strategies to mitigate heat stress and improve human health.[7] Trees and vegetation reduce temperatures through shading, evapotranspiration, and alterations in surface albedo, thereby counteracting the warming effects of climate change.[8] Recent epidemiological evidence demonstrates that higher greenness levels can reduce heat-stress-related mortality, particularly in urban areas.[9] Our previous research also found that enhancing greenness could mitigate a considerable proportion (13%–21%) of heat-related preterm births.[10]

In recent decades, the global landscape has experienced a notable increase in greenness.[11] However, this greening trend is not uniform across all regions,[12] raising questions about the equitable distribution of nature-based solutions for heat mitigation.[13,14] Concurrently, global warming has driven a sharp rise in heat stress, placing a substantial portion of the global population at risk of adverse health conditions.[15] Despite these trends, there has been no global assessment of the co-occurrence of heat stress and greenness changes, limiting our understanding of their combined impact on population health and the inequities in exposure by age, urbanicity, and income status.

To address this knowledge gap, we conduct the first high-resolution global analysis assessing joint exposure to heat stress and greenness at 1 × 1 km resolution from 2000 to 2022. We classified global 1 × 1 km grids into four categories based on trends in heat stress and greenness: (1) increasing heat stress but decreasing greenness (IHDG; the highest-risk category), (2) increasing heat stress and increasing greenness (IHIG), (3) decreasing heat stress and decreasing greenness (DHDG), and (4) decreasing heat stress and increasing greenness (DHIG). By overlaying these exposure categories with age-specific population estimates, we quantified the spatial and temporal patterns of global population exposure to heat stress and greenness dynamics. Our analysis prioritized assessing exposure to IHDG, which represents the most severe scenario for heat mitigation.

MATERIALS AND METHODS

Greenness data acquisition and processing

Greenness was quantified using the normalized difference vegetation index (NDVI), a widely utilized and reliable satellite-based metric. NDVI measures the normalized difference between red and near-infrared reflectance to assess vegetation abundance and vitality.[16] Increases in NDVI values indicate greening, while decreases suggest browning. We utilized the NDVI from the moderate-resolution imaging spectroradiometer (MODIS) Terra data (MOD13A3.061 product) at 1 × 1 km resolution.[12] In each grid for each year during 2000–2022, the yearly maximum NDVI value was used to remove the impacts of seasonality and enable comparable analysis across the globe.

Heat stress data acquisition and processing

We used the universal thermal climate index (UTCI) to measure heat stress, a comprehensive metric that incorporates temperature, solar radiation, wind, and humidity to assess human thermal comfort.[17] The UTCI provides a standardized, globally applicable metric for thermal comfort[18] and is highly sensitive to environmental changes, making it suitable for studying heat stress in diverse climatic and geographic contexts.[19]

In this study, we obtained UTCI data from the European Centre for Medium-Range Weather Forecasts (ECMWF) reanalysis v.5 (ERA5)-HEAT dataset.[20] The ERA5-HEAT dataset offers a spatial resolution of 0.25° × 0.25° (approximately 31 km at the equator) and integrates globally consistent climate reanalysis data. Hourly UTCI values were aggregated to compute daily mean values based on local time zones, which were further processed to generate annual mean values at 1 × 1 km grid level for the period 2000–2022.

Population data

Population data were obtained from WorldPop, providing global population counts and age-specific distributions at 1 × 1 km resolution for 2000–2022.[21] This dataset uses a top-down approach, disaggregating population estimates by age groups (0–1, 5-year intervals up to 80+). We aligned the data with UN population estimates at the country level. Due

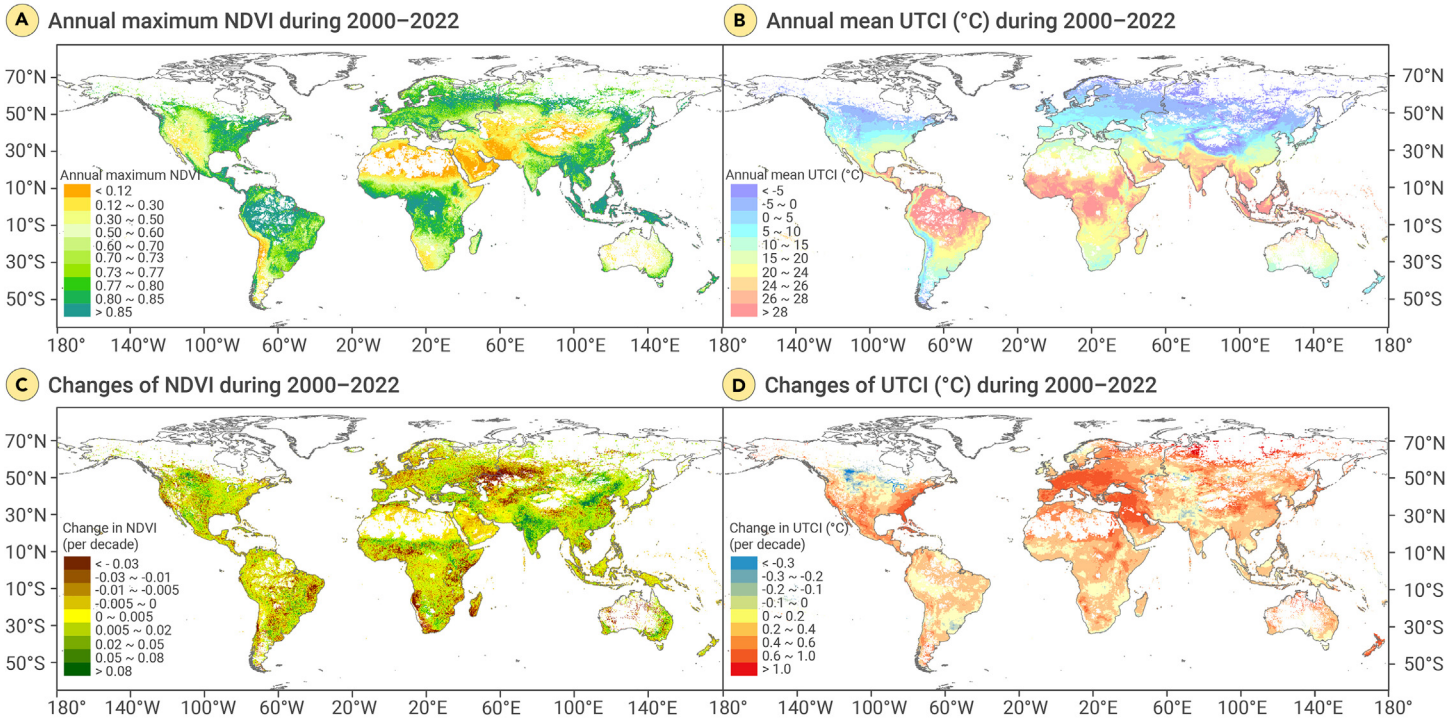

Figure 1. Global distribution and trends of heat stress and greenness (2000–2022) (A and B) Average annual maximum NDVI (A) and average annual mean UTCI (B) across populated areas. (C and D) Changes in annual maximum NDVI (C) and changes in annual mean UTCI (D) from 2000 to 2022. White areas indicate grids without resident populations, which were excluded from analyses. NDVI, normalized difference vegetation index; UTCI, universal thermal climate index.

to the unavailability of data for 2021 and 2022, we used the 2020 total population counts and age-specific population distributions for these years.

Other spatial data

Administrative boundaries were obtained from the Database of Global Administrative Areas (GADM, v.4.1). Gird cells were classified as urban or rural based on Global Human Settlement Layer (GHSL) classification level 1 at 1 × 1 km resolution.[22]

Estimation of trends in heat stress and greenness

Trends in heat stress and greenness were analyzed using the Theil-Sen slope method, a robust non-parametric technique for trend detection.[23,24] This method calculates the median slope of sequential data points, making it robust against outliers.[25] Heat stress trends were adjusted to a 1 × 1 km resolution to match the other datasets. Grid cells were categorized into four exposure categories.

(1) IHDG: positive heat stress slope and negative greenness slope.
(2) IHIG: positive slopes for both.
(3) DHDG: negative slopes for both.
(4) DHIG: negative heat stress slope and positive greenness slope.

Our analysis focuses on IHDG as the primary exposure category, given its critical impact on population health.

Sensitivity analysis

We performed a sensitivity analysis by constraining exposure classifications to statistically significant trends (Mann-Kendall test, $p < 0.05$). The results presented in the supplemental information (Figure S2; Table S5) show that population exposure under this stricter definition closely aligned with our main analyses.

Mapping population exposure profiles

Global population exposure to heat stress and greenness was mapped by integrating exposure categories (IHDG, IHIG, DHDG, and DHIG) with age-specific population estimates. We calculated the total population exposed globally, by continent, and by income group (World Bank classifications: low-income, lower-middle-income, upper-middle-income, and high-income OECD [Organisation for Economic Co-operation and Development] and high-income, non-OECD countries). Urban/rural exposure was identified due to the heightened vulnerabilities of urban populations.[26] Age distributions of exposed populations were compared between 2000–2004 and 2016–2020.

RESULTS

Global trends in heat stress and greenness

Both greenness (measured by annual maximum NDVI) and heat stress (measured by annual mean UTCI) exhibited distinct spatial patterns across regions (Figures 1A and 1B). High greenness levels were observed in East Asia, Southeast Asia, Central Africa, Western Europe, eastern North America, Middle America, the Caribbean, and most of South America. The tropics experience consistently high temperatures year round, with the highest annual heat stress.

From 2000 to 2022, approximately 70% of the global populated areas (i.e., grids with at least one person in 2020) became greener, with pronounced increases in greenness in regions such as India, North and South China, and the Sahel region in Africa (Figure 1C). However, declines in greenness were observed in East and South Africa, Eastern Europe, Central Asia, Brazil, and the Middle East, with notable decreases in Central Asia, East Africa, and Northeast Brazil.

Globally, 98% of populated areas experienced increased heat stress, particularly in the middle and high latitudes of the Northern Hemisphere (Figure 1D). Among these areas experiencing heightened heat stress, approximately 30% coincided with a decline in greenness.

Globally, annual mean heat stress increased from 16.5°C in 2000 to 18.2°C in 2022, while greenness showed a slight rise from 0.58 to 0.59 (Figure 2). All continents experienced increased heat stress, with the most significant rises in Africa (22.7°C–23.7°C), North America (21.6°C–23.0°C), and South America (18.9°C–20.0°C). Despite the global upward trend, Asia saw a notable increase in greenness (0.44–0.48), while Africa (0.60–0.59) and North America (0.70–0.69) experienced slight declines over the period studied.

Substantial disparities were observed across income groups (Figure 2; Table S1). Upper-middle-income, lower-middle-income, and low-income countries experienced significant increases in heat stress, with upper-middle-income countries rising from 15.2°C to 17.1°C, lower-middle-income countries from 19.8°C to 21.0°C, and low-income countries from 22.9°C to 23.9°C. Upper-middle-income countries also saw declines in greenness, while high-income countries maintained relatively stable trends. High-income OECD countries had lower

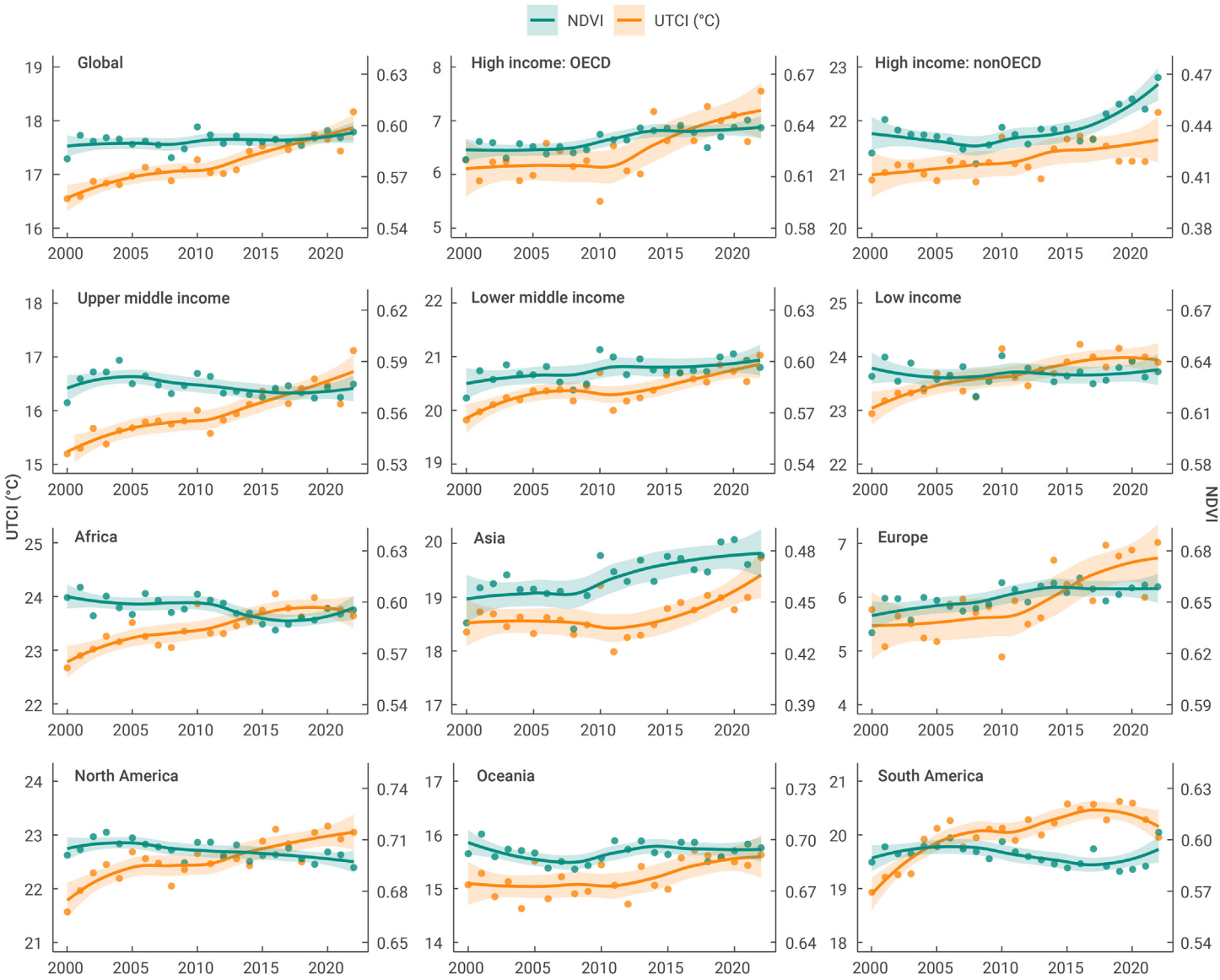

Figure 2. Trends in population-weighted mean annual maximum NDVI and annual mean UTCI (2000–2022) Global trends and trends by income group and continent. Point estimates represent raw data, and curves and error ribbons show locally estimated scatterplot smoothing (LOESS) fits. NDVI, normalized difference vegetation index; UTCI, universal thermal climate index; OECD, Organisation for Economic Co-operation and Development.

heat stress levels (6.3°C in 2000 to 7.5°C in 2022) and higher greenness (0.62–0.64), whereas high-income, non-OECD countries showed slight increases in heat stress (20.9°C–22.2°C) and greenness (0.42–0.47).

Global spatial distributions of IHDG exposure

Approximately 69.3% of global populated areas (57 million km^2) were identified as experiencing IHDG. In contrast, only 29.1% of populated areas (~24 million km^2) exhibited IHIG, while 1.2% (~1 million km^2) experienced DHDG and 0.3% (~0.3 million km^2) showed DHIG (Figure 3A).

Our analysis revealed that 41.3% of the global population (~2,909 million individuals) was exposed to IHDG conditions, with 74% (~2,142 million) residing in urban areas. In contrast, 56.3% (~3,969 million) experienced IHIG, 1.5% (106 million) was exposed to DHDG, and 0.9% (~62 million) had DHIG (Table S2).

Spatial patterns of IHDG exposure highlighted specific subregions with high exposure (Figures 3B–3H). Notable areas included the East Coast of the United States, Western Europe, Western Africa, and Eastern China.

Asia had the highest number of people exposed to IHDG (1,366 million), followed by Africa (707 million), Europe (290 million), North America (281 million), South America (249 million), and Oceania (16 million) (Figure 4). Urban populations accounted for the majority of exposures, with 1,119 million in Asia, 413 million in Africa, 188 million in Europe, 220 million in North America, 192 million in South America, and 11 million in Oceania.

Africa had the highest proportion of urban populations exposed to IHDG (68.6%), followed by South America (61.7%), North America (51.2%), Asia (47.0%), Oceania (42.5%), and Europe (40.0%). Middle-income countries bore the greatest burden, accounting for 74.9% of the global total exposed population (2,168 million) and 79.1% of the exposed urban population (1,687 million). Over 50% of the urban populations in LMICs were exposed to IHDG: low-income countries (59.6%), lower-middle-income countries (56.8%), and upper-middle-income countries (51.3%).

Further analysis of disparities between IHDG and IHIG populations revealed that IHDG populations were more disadvantaged across income groups (Table S3). In high-income countries, 15.1% of the population was exposed to IHDG, compared to 26.1% for IHIG. Conversely, lower-middle-income regions had a larger proportion of IHDG exposure (36.8%) compared to IHIG (27.4%), and low-income countries showed a similar pattern (5.9% for IHDG vs. 4.0% for IHIG).

Age distribution of global population exposure

We observed an accelerated aging trend in populations exposed to IHDG compared to those unexposed (Figure 5; Table S4). From 2000–2004 to 2016–2020, the proportion of older adults (≥65 years) exposed to IHDG increased from 6.8% (106 of 1,558 million) to 11.8% (210 of 1,778 million), a 97% rise. Among non-IHDG populations, the proportion of older adults increased

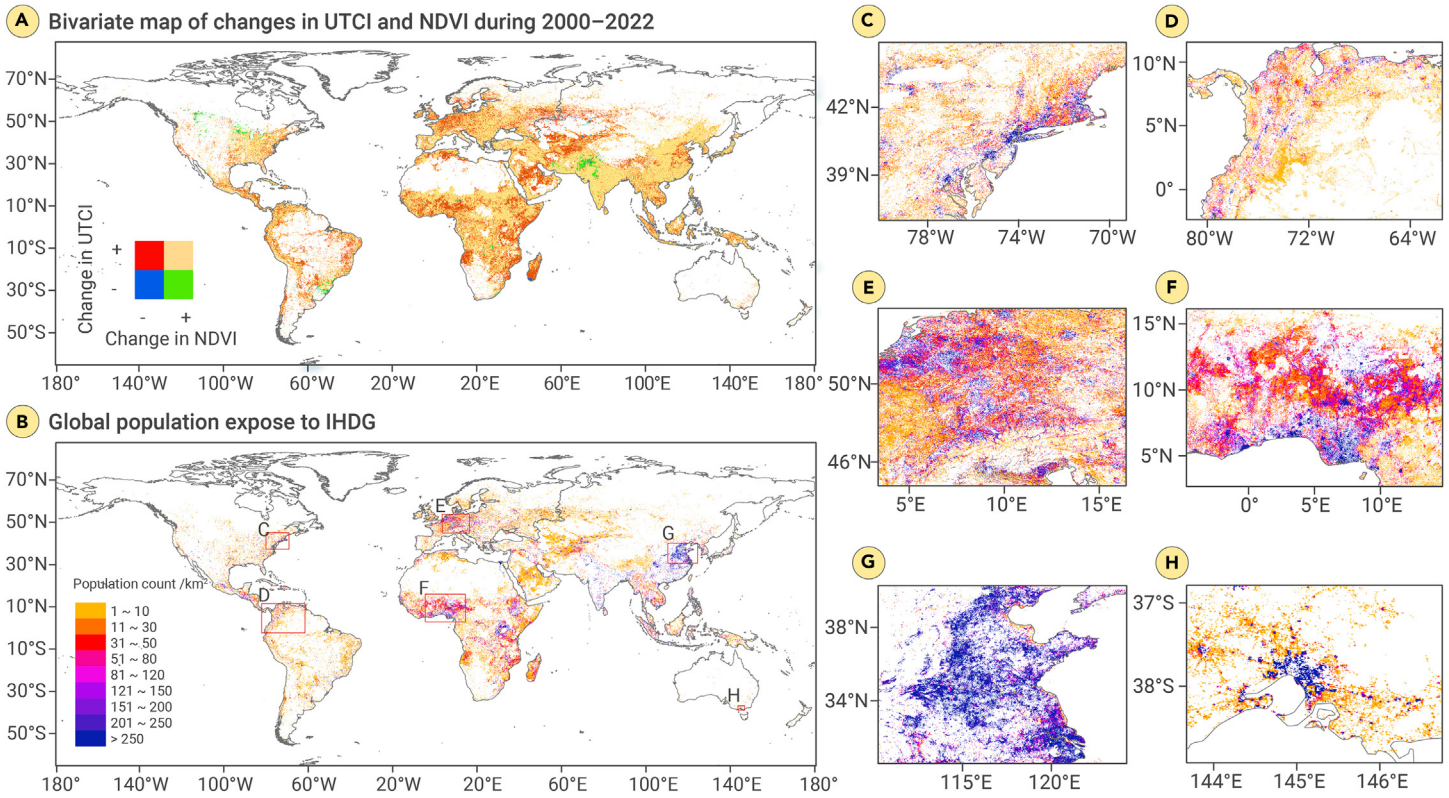

Figure 3. Global distribution of IHDG exposure and population exposure hotspots (A) Bivariate map of changes in UTCI and NDVI. (B) Global distribution of populations exposed to IHDG. (C–H) Zoomed-in views of subregions with relative high exposure within each continent: East Coast of the United States (C), northern South America (D), Western Europe (E), Western Africa (F), East China (G), and Victoria, Australia (H). NDVI, normalized difference vegetation index; UTCI, universal thermal climate index; IHDG, increasing heat stress but decreasing greenness.

from 7.6% (366 of 4,822 million) to 8.5% (527 of 6,189 million), a 44% increase. This pattern was consistently observed across all continents. Further analysis revealed similar disparities in aging trends between IHDG and IHIG populations. The IHDG group had higher proportions of older adults, with 4.16% aged 65–69 compared to 3.29% for IHIG and 2.65% aged 80 and above compared to 1.75% for IHIG (Figure S1; Table S3).

DISCUSSION

This study provided the first global, high-resolution assessment of joint population exposure to heat stress and greenness trends over the past two decades. Our findings reveal a consistent increase in heat stress globally, particularly in Europe and South America. While global greenness increased overall, declines were observed in some regions of Africa and the Americas. Critically, the increase in greenness did not adequately mitigate rising heat stress, with approximately 69.3% of populated areas and 41.3% of the global population exposed to IHDG conditions. Urban areas and proportions experienced disproportionately higher IHDG exposure, and populations exposed to IHDG had a much faster pace of population aging.

Our findings align with previous observations on increasing heat stress[27–29] but extend this understanding by integrating greenness trends. The scale of IHDG exposure underscores the urgent need for actions to address this environmental and public health challenge in a warming climate. Urban areas, where heat stress and reduced greenness are exacerbated by the urban heat island effect and higher population densities,[30,31] require particular attention.

Nature-based solutions, such as increasing greenness and expanding urban green infrastructure, have been framed and identified to mitigate and adapt to climate change.[32,33] Our findings emphasizes the importance of implementing targeted interventions and policies to mitigate the adverse health effects of heat stress in IHDG regions.[34] However, even in regions with increasing greenness (e.g., IHIG), the benefits of greenness may be limited if temperature increases outpace the greenness expansion. In such cases, additional policy interventions are still needed to enhance the effectiveness of greenness in mitigating heat stress.

Substantial regional disparities in heat stress and greenness changes were observed. Hotspots of IHDG, such as regions in Africa and South America, exhibited greater changes of heat stress and greenness, with deforestation, conversion for agriculture, and urban expansion emerging as key drivers of greenness loss.[35] Initiatives like the Great Green Wall in Africa[36] and the Three-North Shelter Forest Program in China[37] demonstrate the potential of targeted interventions to combat environmental degradation and climate change effects.

Our assessment revealed socioeconomic disparities in heat stress, greenness changes, and IHDG exposure. LMICs, particularly those in hot and dry regions, bore the greatest burden due to infrastructure development, urbanization, and population growth.[38] Additionally, populations exposed to IHDG experienced a faster aging trend than unexposed populations, highlighting the vulnerability of older adults to climate-related stress. Physiological, social, and economic factors, such as reduced thermoregulatory capacity and limited access to resources, exacerbate this vulnerability.[39,40]

This study has several limitations. First, the NDVI was used as a proxy for greenness, which may be affected by the misrepresentation of aerosols in surface reflectance products, particularly over arid and bright surfaces.[41] However, this is unlikely to significantly bias population exposure estimates, as these regions are generally sparsely populated or uninhabited. Second, the NDVI does not differentiate between types of green spaces, such as natural landscapes, urban parks, or agricultural areas, which may have varying effects on temperature regulation and heat stress mitigation.[42,43] Third, our analysis does not account for socioeconomic factors, such as access to resources, healthcare, and housing materials, which influence vulnerability to heat stress. These limitations highlight the need for future research to explore more nuanced measures of greenness and incorporate socioeconomic data.

In conclusion, this global study highlights that spatiotemporal trends of global greenness have not aligned with the population's heat mitigation needs, leaving billions exposed to increasing heat stress and declining greenness. The disproportionate burden on urban populations, LMICs, and aging communities underscores the urgent need for targeted interventions. There is significant potential to reduce heat stress and its adverse health impacts by enhancing greenness, particularly in IHDG exposure. Our findings provide a scientific foundation for

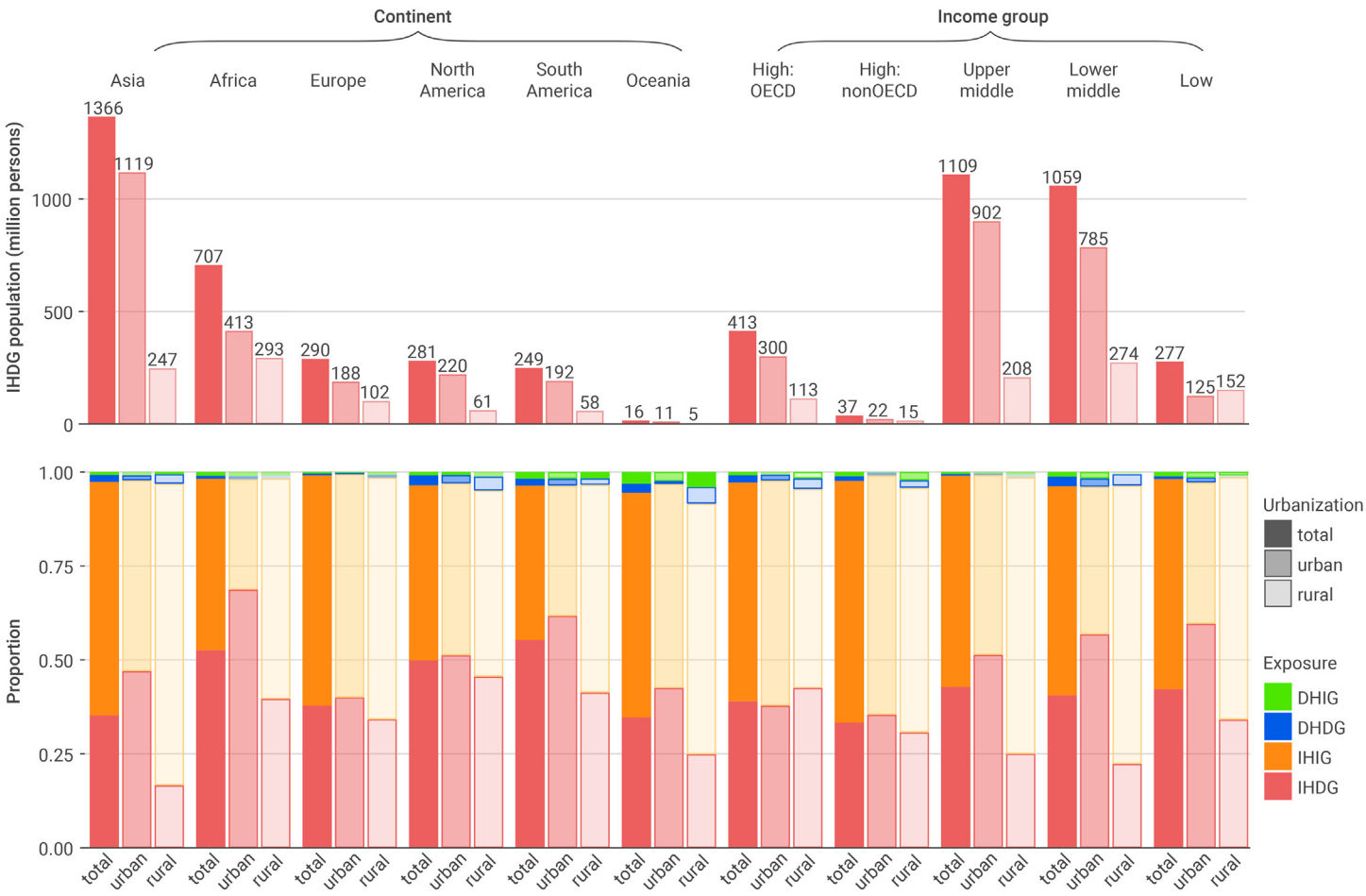

Figure 4. Population exposure to heat stress and greenness by continent and income group Numbers and proportions of populations exposed to different categories (IHDG, IHIG, DHDG, and DHIG) in total, urban, and rural areas. OECD, Organisation for Economic Co-operation and Development; IHDG, increasing stress but decreasing greenness; IHIG, increasing heat stress and increasing greenness; DHDG, decreasing heat stress and decreasing greenness; DHIG, decreasing heat stress and increasing greenness.

policymakers and urban planners to implement evidence-based solutions that safeguard public health in an era of increasing heat stress.

DATA AND CODE AVAILABILITY

Data of heat stress, greenness, and global populations are available for free from ERA5-HEAT (https://cds.climate.copernicus.eu/cdsapp#!/dataset/derived-utci-historical?tab=overview), MODIS vegetation index products (https://modis.gsfc.nasa.gov/data/dataprod/mod13.php), and WorldPop (https://www.worldpop.org/datacatalog/), respectively. Analysis codes are available from the corresponding authors upon request and will be shared on https://github.com/pipty/Global_Pop_Exposed_IHDG.

REFERENCES

1. Perkins-Kirkpatrick, S.E. and Lewis, S.C. (2020). Increasing trends in regional heatwaves. *Nat. Commun.* **11**:3357. DOI:https://doi.org/10.1038/s41467-020-16970-7.
2. Romanello, M., Napoli, C.D., Green, C. et al. (2023). The 2023 report of the Lancet Countdown on health and climate change: the imperative for a health-centred response in a world facing irreversible harms. *Lancet* **402**:2346–2394. DOI:https://doi.org/10.1016/S0140-6736(23)01859-7.
3. Zhao, Q., Guo, Y., Ye, T. et al. (2021). Global, regional, and national burden of mortality associated with non-optimal ambient temperatures from 2000 to 2019: a three-stage modelling study. *Lancet Planet. Health* **5**:e415–e425. DOI:https://doi.org/10.1016/S2542-5196(21)00081-4.
4. Hansen, A., Bi, P., Nitschke, M. et al. (2011). Older persons and heat-susceptibility: the role of health promotion in a changing climate. *Health Promot. J. Aust.* **22**:17–20.
5. Hajat, S. and Kosatky, T. (2010). Heat-related mortality: a review and exploration of heterogeneity. *J. Epidemiol. Community Health* **64**:753–760. DOI:https://doi.org/10.1136/jech.2009.087999.
6. Li, D. and Bou-Zeid, E. (2013). Synergistic Interactions between Urban Heat Islands and Heat Waves: The Impact in Cities Is Larger than the Sum of Its Parts. *J. Appl. Meteorol. Climatol.* **52**:2051–2064. DOI:https://doi.org/10.1175/JAMC-D-13-02.1.
7. Romanello, M., Di Napoli, C., Drummond, P. et al. (2022). The 2022 report of the Lancet Countdown on health and climate change: health at the mercy of fossil fuels. *Lancet* **400**:1619–1654. DOI:https://doi.org/10.1016/S0140-6736(22)01540-9.
8. Peng, S., Piao, S., Ciais, P. et al. (2012). Surface urban heat island across 419 global big cities. *Environ. Sci. Technol.* **46**:696–703. DOI:https://doi.org/10.1021/es2030438.
9. Zhang, H., Liu, L., Zeng, Y. et al. (2021). Effect of heatwaves and greenness on mortality among Chinese older adults. *Environ. Pollut.* **290**:118009. DOI:https://doi.org/10.1016/j.envpol.2021.118009.
10. Ye, T., Guo, Y., Huang, W. et al. (2024). Heat Exposure, Preterm Birth, and the Role of Greenness in Australia. *JAMA Pediatr.* **178**:376–383. DOI:https://doi.org/10.1001/jamapediatrics.2024.0001.
11. Ding, Z., Peng, J., Qiu, S. et al. (2020). Nearly Half of Global Vegetated Area Experienced Inconsistent Vegetation Growth in Terms of Greenness, Cover, and Productivity. *Earths Future* **8**:e2020EF001618. https://doi.org/10.1029/2020ef001618.
12. Pan, N., Feng, X., Fu, B. et al. (2018). Increasing global vegetation browning hidden in overall vegetation greening: Insights from time-varying trends. *Rem. Sens. Environ.* **214**:59–72. DOI:https://doi.org/10.1016/j.rse.2018.05.018.
13. Matthew McConnachie, M. and Shackleton, C.M. (2010). Public green space inequality in small towns in South Africa. *Habitat Int.* **34**:244–248. DOI:https://doi.org/10.1016/j.habitatint.2009.09.009.
14. Mitchell, R. and Popham, F. (2008). Effect of exposure to natural environment on health inequalities: an observational population study. *Lancet* **372**:1655–1660. DOI:https://doi.org/10.1016/S0140-6736(08)61689-X.
15. Kovats, R.S. and Hajat, S. (2008). Heat stress and public health: a critical review. *Annu. Rev. Publ. Health* **29**:41–55. DOI:https://doi.org/10.1146/annurev.publhealth.29.020907.090843.
16. Sadeh, M., Brauer, M., Dankner, R. et al. (2021). Remote sensing metrics to assess exposure to residential greenness in epidemiological studies: A population case study from the Eastern Mediterranean. *Environ. Int.* **146**:106270. DOI:https://doi.org/10.1016/j.envint.2020.106270.
17. Jendritzky, G., de Dear, R. and Havenith, G. (2012). UTCI—Why another thermal index? *Int. J. Biometeorol.* **56**:421–428. DOI:https://doi.org/10.1007/s00484-011-0513-7.
18. Blazejczyk, K., Epstein, Y., Jendritzky, G. et al. (2012). Comparison of UTCI to selected thermal indices. *Int. J. Biometeorol.* **56**:515–535. DOI:https://doi.org/10.1007/s00484-011-0453-2.
19. Krüger, E.L. (2021). Literature Review on UTCI Applications. In Applications of the Universal Thermal Climate Index UTCI in Biometeorology: Latest Developments and Case Studies, E.L.

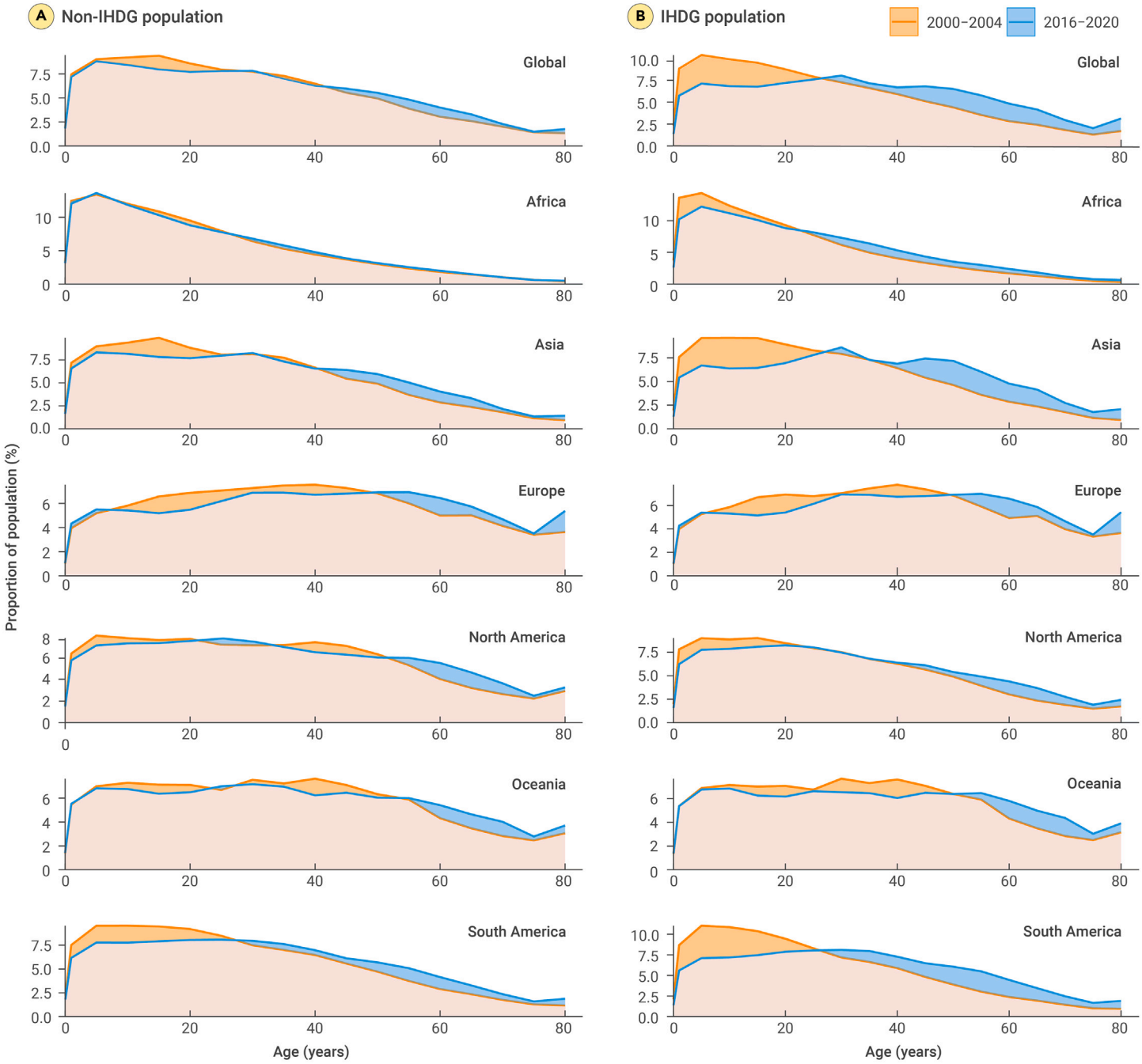

Figure 5. Age distribution of populations exposed and unexposed to IHDG (2000–2004 vs. 2016–2020) Unexposed populations (A) and populations exposed to IHDG (B). IHDG, increasing heat stress but decreasing greenness.

Krüger, ed. (Springer International Publishing), pp. 23–65. DOI:https://doi.org/10.1007/978-3-030-76716-7_3.

20. Di Napoli, C., Barnard, C., Prudhomme, C. et al. (2020). ERA5-HEAT: A global gridded historical dataset of human thermal comfort indices from climate reanalysis. *Geoscience Data Journal* **8**:2–10. DOI:https://doi.org/10.1002/gdj3.102.
21. Lloyd, C.T., Chamberlain, H., Kerr, D. et al. (2019). Global spatio-temporally harmonised datasets for producing high-resolution gridded population distribution datasets. *Big Earth Data* **3**:108–139. DOI:https://doi.org/10.1080/20964471.2019.1625151.
22. Schiavina, M., Melchiorri, M. and Pesaresi, M. (2023). GHS-SMOD R2023A–GHS Settlement Layers, Application of the Degree of Urbanisation Methodology (Stage I) to GHS-POP R2023A and GHS-BUILT-S R2023A, Multitemporal (1975–2030), **20** (European Commission, Joint Research Centre (JRC)). DOI:https://doi.org/10.2905/A0DF7A6F-49DE-46EA-9BDE-563437A6E2BA.
23. Theil, H. (1992). A Rank-Invariant Method of Linear and Polynomial Regression Analysis. In Henri Theil's Contributions to Economics and Econometrics: Econometric Theory and Methodology, B. Raj and J. Koerts, eds. (Netherlands: Springer), pp. 345–381. DOI:https://doi.org/10.1007/978-94-011-2546-8_20.
24. Sen, P.K. (1968). Robustness of Some Nonparametric Procedures in Linear Models. *Ann. Math. Stat.* **39**:1913–1922.
25. Fernandes, R. and G. Leblanc, S. (2005). Parametric (modified least squares) and non-parametric (Theil–Sen) linear regressions for predicting biophysical parameters in the presence of measurement errors. *Rem. Sens. Environ.* **95**:303–316. DOI:https://doi.org/10.1016/j.rse.2005.01.005.
26. Ebi, K.L., Capon, A., Berry, P. et al. (2021). Hot weather and heat extremes: health risks. *Lancet* **398**:698–708. DOI:https://doi.org/10.1016/S0140-6736(21)01208-3.
27. Program, C.C.S. and Karl, T. (2006). Temperature Trends in the Lower Atmosphere: Steps for Understanding and Reconciling Differences: Report (US Climate Change Science Program).
28. Kerr, R.A. (2007). Global Warming Is Changing the World. *Science* **316**:188–190. DOI:https://doi.org/10.1126/science.316.5822.188.
29. Marengo, J.A., Jones, R., Alves, L.M. et al. (2009). Future change of temperature and precipitation extremes in South America as derived from the PRECIS regional climate modeling system. *Int. J. Climatol.* **29**:2241–2255. DOI:https://doi.org/10.1002/joc.1863.
30. Leal Filho, W., Echevarria Icaza, L., Neht, A. et al. (2018). Coping with the impacts of urban heat islands. A literature based study on understanding urban heat vulnerability and the

need for resilience in cities in a global climate change context. *J. Clean. Prod.* **171**:1140–1149. DOI:https://doi.org/10.1016/j.jclepro.2017.10.086.
31. Li, Y., Schubert, S., Kropp, J.P. et al. (2020). On the influence of density and morphology on the Urban Heat Island intensity. *Nat. Commun.* **11**:2647. DOI:https://doi.org/10.1038/s41467-020-16461-9.
32. MacKinnon, K., Sobrevila, C. and Hickey, V. (2008). Biodiversity, Climate Change, and Adaptation: Nature-Based Solutions from the World Bank Portfolio (The World Bank).
33. Bauduceau, N., Berry, P., Cecchi, C. et al. (2015). Towards an EU research and innovation policy agenda for nature-based solutions & re-naturing cities: Final report of the horizon 2020 expert group on'nature-based solutions and re-naturing cities' (Publications Office of the European Union, Place of Publication: Bruxelles), p. 76. DOI:https://doi.org/10.2777/479582.
34. Lemonsu, A., Viguié, V., Daniel, M. et al. (2015). Vulnerability to heat waves: Impact of urban expansion scenarios on urban heat island and heat stress in Paris (France). *Urban Clim.* **14**:586–605. DOI:https://doi.org/10.1016/j.uclim.2015.10.007.
35. Sy, V.D., Herold, M., Achard, F. et al. (2015). Land use patterns and related carbon losses following deforestation in South America. *Environ. Res. Lett.* **10**:124004. DOI:https://doi.org/10.1088/1748-9326/10/12/124004.
36. Mirzabaev, A., Sacande, M., Motlagh, F. et al. (2022). Economic efficiency and targeting of the African Great Green Wall. *Nat. Sustain.* **5**:17–25. DOI:https://doi.org/10.1038/s41893-021-00801-8.
37. Zhai, J., Wang, L., Liu, Y. et al. (2023). Assessing the effects of China's Three-North Shelter Forest Program over 40 years. *Sci. Total Environ.* **857**:159354. DOI:https://doi.org/10.1016/j.scitotenv.2022.159354.
38. Angel, S., Parent, J., Civco, D.L. et al. (2011). The dimensions of global urban expansion: Estimates and projections for all countries, 2000–2050. *Prog. Plann.* **75**:53–107. DOI:https://doi.org/10.1016/j.progress.2011.04.001.
39. Meade, R.D., Akerman, A.P., Notley, S.R. et al. (2020). Physiological factors characterizing heat-vulnerable older adults: A narrative review. *Environ. Int.* **144**:105909. DOI:https://doi.org/10.1016/j.envint.2020.105909.
40. Wolf, J., Adger, W.N., Lorenzoni, I. et al. (2010). Social capital, individual responses to heat waves and climate change adaptation: An empirical study of two UK cities. *Glob. Environ. Change* **20**:44–52. DOI:https://doi.org/10.1016/j.gloenvcha.2009.09.004.
41. Didan, K., Munoz, A.B., Solano, R. et al. (2015). MODIS vegetation index user's guide (MOD13 series), **35** (University of Arizona: Vegetation Index and Phenology Lab), pp. 2–33.
42. Iungman, T., Cirach, M., Marando, F. et al. (2023). Cooling cities through urban green infrastructure: a health impact assessment of European cities. *Lancet* **401**:577–589. DOI:https://doi.org/10.1016/S0140-6736(22)02585-5.
43. Van Ryswyk, K., Prince, N., Ahmed, M. et al. (2019). Does urban vegetation reduce temperature and air pollution concentrations? Findings from an environmental monitoring study of the Central Experimental Farm in Ottawa, Canada. *Atmos. Environ.* **218**:116886. DOI:https://doi.org/10.1016/j.atmosenv.2019.116886.

ACKNOWLEDGMENTS

This study was supported by the Australian Research Council (DP210102076) and the Australian National Health and Medical Research Council (NHMRC; GNT2000581); YG by the Leader Fellowship (GNT2008813) of the Australian National Health and Medical Research Council; SL by an Emerging Leader Fellowship of the Australian National Health and Medical Research Council (GNT2009866); TY, YW, BW, and WH by the China Scholarship Council (grant nos. 201906320051, 202006010044, 202006010043, and 202006380055, respectively); PY by Monash Faculty of Medicine, Nursing and Health Sciences (FMNHS) Early Career Postdoctoral Fellowships 2023; YZ by an NHMRC e-Asia Joint Research Program Grant (GNT2000581); and ZY and WY by a Monash Graduate Scholarship and Monash International Tuition Scholarship. The funders had no role in the study design, data collection and analysis, decision to publish, or preparation of the manuscript. We thank Zhihu Xu and Shuang Zhou for their valuable suggestions on figure revisions during the revision process.

AUTHOR CONTRIBUTIONS

Conceptualization, R.X. and T.Y.; methodology, T.Y. and R.X.; data collection, T.Y.; analyses, T.Y.; visualization, T.Y.; supervision, S.L., M.J.A., and Y.G.; writing – original draft, T.Y.; writing – review & editing, all authors. All authors contributed to the manuscript and approved the final version.

DECLARATION OF INTERESTS

M.J.A. holds investigator-initiated grants from Pfizer, Boehringer-Ingelheim, Sanofi, and GSK for unrelated research. He has undertaken an unrelated consultancy for Sanofi. He also received a speaker's fee from GSK.

SUPPLEMENTAL INFORMATION

It can be found online at https://doi.org/10.1016/j.xinn.2025.100870.